Acta Crystallographica Section D
Biological Crystallography
ISSN 0907-4449

Comparison of phasing methods for sulfur-SAD using in-house chromium radiation: case studies for standard proteins and a 69 kDa protein

Nobuhisa Watanabe,[a]* Yu Kitago,[a] Isao Tanaka,[a] Jia-wei Wang,[b] Yuan-xin Gu,[b] Chao-de Zheng[b] and Hai-fu Fan[b]

[a]Graduate School of Science, Hokkaido University, Sapporo 0600810, Japan, and [b]Institute of Physics, Chinese Academy of Sciences, Beijing 100080, People's Republic of China

Correspondence e-mail: nobuhisa@sci.hokudai.ac.jp

Received 2 May 2005
Accepted 9 September 2005

Phasing of the crystal structures of four standard proteins (lysozyme, trypsin, glucose isomerase and thaumatin) and a novel 69 kDa protein from *Thermus thermophilus*, TT0570, was performed using the single-wavelength anomalous diffraction of S atoms intrinsically present within the native protein molecules. To utilize the sulfur anomalous diffraction, the data sets were collected using the loopless data-collection method with chromium $K\alpha$ X-rays of wavelength 2.29 Å. Three phasing methods, *MLPHARE*, *SHARP* and *OASIS*-2004, were tested in combination with the *DM* or *SOLOMON* density-modification method. The results showed that the solvent contents are still an important factor for phasing with the S-SAD method, even when longer wavelength Cr $K\alpha$ radiation is used. Of the three procedures, the improved direct phasing of *OASIS*-2004 with its implemented fragment feedback to the direct-method probability calculation gave the best results in determining the initial phases. For all five proteins, almost the entire models could be built automatically.

1. Introduction

In the last decade, the multi-wavelength anomalous diffraction (MAD) method (Hendrickson, 1985) in conjunction with selenomethionine derivatization has become a powerful and commonly used tool to solve novel protein structures. In addition to selenium, many other anomalous scatterers have also been incorporated into protein molecules for phasing (Dauter *et al.*, 2000; Nagem *et al.*, 2001; Evans & Bricogne, 2002; Usón *et al.*, 2003). In most cases, MAD phases provide electron-density maps of excellent quality immediately after data collection. However, the MAD method requires synchrotron X-rays to measure the intensities at different wavelengths in order to utilize the anomalous differences of heavy atoms such as Se, Pt, Au, Hg *etc.* On the other hand, single-wavelength anomalous diffraction (SAD) phasing at the peak wavelength of such heavy atoms (Rice *et al.*, 2000) is also becoming increasingly common. The SAD method makes more efficient use of beam time and reduces the extent of radiation damage. A new technique that utilizes longer wavelength X-rays for phasing (Stuhrmann *et al.*, 1995; Chayen *et al.*, 2000; Liu *et al.*, 2000; Cianci *et al.*, 2001; Weiss *et al.*, 2001; Micossi *et al.*, 2002; Ramagopal *et al.*, 2003) provided the possibility of using in-house Cr $K\alpha$ radiation (2.29 Å), which was first reported by Blow (1958). The choice of X-ray wavelength is one of the major decisions required for SAD data collection. The decision is made following evaluation of several wavelength-dependent factors and data-processing

Table 1
Crystallization conditions and contents of the unit cell for the sample proteins.

	Crystallization condition (cryoprotectant)	Residues per asymmetric unit	Anomalous scatterers per molecule†	Estimated $\langle\lvert\Delta F\rvert\rangle/\langle F\rangle$ (%)	Solvent content (%)	Anomalous scatterer sites used for phasing
Lysozyme	60 mg ml^{-1} protein, 0.1 *M* sodium acetate pH 4.2, 2.0 *M* NaCl (30% glycerol)	129	10 S (4 SS), 8 Cl^-	5.1	38.2	16
Trypsin	60 mg ml^{-1} protein, 0.1 *M* Tris–HCl pH 7.8, 0.2 *M* $LiSO_4$, 25% PEG 4000, 16% glycerol	223	14 S (6 SS), 1 Ca^{2+}, 1 Zn^{2+}	4.2	37.9	15
Thaumatin	30 mg ml^{-1} protein, 0.1 *M* Na_2ADA/NaADA pH 6.5, 0.8 *M* K,Na tartrate (30% glycerol)	207	17 S (8 SS)	2.5	55.7	16
Glucose isomerase	15 mg ml^{-1} protein, 0.05 *M* Tris–HCl pH 7.0, 11% MPD, 0.1 *M* $MgCl_2$ (30% MPD)	388	9 S	1.2	53.7	8
TT0570	10 mg ml^{-1} protein, 0.2 *M* $Mg(NO_3)_2$, 20% PEG 3350 (15% PEG 400)	1206 (603 × 2)	11 S	1.1	48.0	20

† SS, super-sulfur or disulfide.

methods (Teplyakov *et al.*, 1998; Mueller-Dieckmann *et al.*, 2004). Use of a wavelength of 2.1 Å was suggested as the best choice to obtain the highest anomalous signal-to-noise ratio using standard means of data collection and processing (Mueller-Dieckmann *et al.*, 2005). However, changing the wavelength is not possible for in-house X-ray sources. We may only choose from Cu $K\alpha$ (1.54 Å), Co $K\alpha$ (1.79 Å) and Cr $K\alpha$ (2.29 Å) as an anticathode target for longer wavelengths in the laboratory.

Phasing using the anomalous signal of sulfur alone was first reported in the structure analysis of crambin (Hendrickson & Teeter, 1981) using Cu $K\alpha$ X-rays. Despite this accomplishment, there has only been a revival in interest in the use of sulfur anomalous signal in the past few years. To utilize the anomalous signal from light atoms such as sulfur, it is advantageous to perform data collection using the longer wavelength of Cr $K\alpha$ radiation where the anomalous intensity difference or the Bijvoet ratio becomes 1–2% of the total reflection intensity, because the $\Delta f''$ value of sulfur becomes 1.14 e^- at 2.29 Å compared with 0.56 e^- at 1.54 Å, as suggested by Wang (1985). Successful applications of the sulfur SAD (S-SAD) technique have been reported using a longer wavelength from a chromium target (Chen *et al.*, 2004; Phillips *et al.*, 2004; Rose *et al.*, 2004; Madauss *et al.*, 2004) with an X-ray apparatus optimized for protein crystallography (Yang *et al.*, 2003).

Recently, the use of selenomethionine-derivatized protein in combination with Cr $K\alpha$ radiation has been proposed as an efficient routine pathway for in-house high-throughput protein crystallography (Xu *et al.*, 2005). However, using S atoms as anomalous scatterers has the advantage that the S atoms are naturally present in proteins as methionine or cysteine residues and thus neither modification nor heavy-atom soaking is necessary for structure analysis. The average frequency of S atoms in 24 bacterial proteomes is 3.3 sulfurs per 100 amino acids (Jáuregui *et al.*, 2000; Micossi *et al.*, 2002) and genomic scale analysis shows that many gene products of bacterial genomes will have a Bijvoet difference higher than 1.5% with Cr $K\alpha$ radiation (Nagem *et al.*, 2005). Higher sulfur contents are expected in eukaryotic genomes (Micossi *et al.*, 2002).

In the case of light atoms such as sulfur, the Bijvoet difference is still very small even when a longer wavelength is used. Therefore, highly accurate data collection and powerful methods for determining initial phases from the diffraction data are essential. One of the experimental difficulties in using longer wavelengths is the increased absorption. In standard protein crystallography where the crystal is mounted in a cryoloop with cryobuffer, X-ray absorption by these materials sometimes prevents the detection of tiny anomalous signals. We have developed a novel technique for mounting a protein crystal to eliminate absorption by the cryobuffer and cryoloop and have demonstrated its superiority to the standard cryoloop method (Kitago *et al.*, 2005). This technique increases the precision of the anomalous differences between the Bijvoet pair and makes the in-house S-SAD method with a Cr $K\alpha$ X-ray source a very useful tool for high-throughput structure determination.

However, the solvent fraction is an important factor in S-SAD phasing, as mentioned by Ramagopal *et al.* (2003). In this study, several proteins with different Bijvoet differences and solvent contents were chosen as test proteins and three phasing methods were compared, *OASIS*-2004 (Wang, Chen, Gu, Zheng, Jiang *et al.*, 2004; Wang, Chen, Gu, Zheng & Fan, 2004), *SHARP* (de La Fortelle & Bricogne, 1997) and *MLPHARE* (Otwinowski, 1991), in combination with density improvement by *DM* (Cowtan, 1994) or *SOLOMON* (Abrahams & Leslie, 1996) and auto-model building by *RESOLVE*

Table 2
Diffraction data statistics for the sample data.

	Lysozyme	Trypsin	Thaumatin	Glucose isomerase	TT0570
Unit-cell parameters (Å)	a = 78.4, c = 37.0	a = 54.6, c = 107.3	a = 57.9, c = 150.3	a = 92.8, b = 98.1, c = 102.6	a = 100.3, b = 109.0, c = 114.6
Space group	$P4_32_12$	$P3_121$	$P4_12_12$	$I222$	$P2_12_12$
Resolution limit	50.0–2.17 (2.25–2.17)	50.0–2.17 (2.25–2.17)	50.0–2.17 (2.25–2.17)	50.0–2.17 (2.25–2.17)	50.0–2.17 (2.25–2.17)
Reflections measured	301531	196655	704259	675807	1732599
Oscillation angle (°)	1.0	1.0	0.5	1.0	0.5
Total rotation range (°)	720	360	720	720	720
Unique reflections	6383	10388	14202	47046	66273
Completeness (%)	98.3 (85.8)	100.0 (99.9)	99.4 (95.2)	98.4 (93.0)	98.6 (87.7)
Mosaicity (°)	0.88	0.55	0.44	0.46	0.75
R_{sym}† (%)	4.0 (12.3)	5.6 (12.6)	6.4 (13.7)	5.4 (16.8)	8.0 (29.2)
$R_{p.i.m.}$‡ (%)	0.6 (2.1)	1.3 (3.4)	0.9 (2.3)	1.1 (3.6)	1.5 (7.8)
$\langle\Delta F\rangle/\langle F\rangle$ (%)	3.2 (5.3)	3.0 (5.2)	2.8 (4.3)	2.5 (7.5)	1.9 (10.7)
Multiplicity§	47.2 (36.0)	18.9 (14.1)	49.6 (38.8)	27.4 (21.5)	26.1 (17.3)
$\langle I\rangle/\langle\sigma(I)\rangle$	104.3 (35.0)	60.3 (26.0)	107.4 (59.0)	36.0 (9.2)	44.4 (7.3)

† $R_{sym} = \sum|I - \langle I\rangle|/\sum I$. ‡ $R_{p.i.m.}$ is the precision-indicating merging R factor (Weiss & Hilgenfeld, 1997). § Counts Friedel mates as the same reflection.

(BUILD only; Terwilliger, 2003*a*,*b*) and/or *ARP*/*wARP* (Perrakis *et al.*, 1999).

2. Methods

2.1. Sample preparation, diffraction data collection and processing

Hen egg-white lysozyme (Seikagaku Kogyo, catalogue No. 100940), bovine pancreas trypsin (Sigma, catalogue No. T7309), *Thaumatinococcus daniellii* thaumatin (Sigma, catalogue No. T7638) and *Streptomyces rubiginosus* glucose isomerase (Hampton Research, catalogue No. HR7-100) were purchased and used without further purification. Assuming Cr $K\alpha$ X-ray wavelength, the overall Bijvoet difference or $\langle|\Delta F|\rangle/\langle F\rangle$ values calculated from the amino-acid sequence and all other possible anomalous scatterers in the crystals were 5.1, 4.2, 2.5 and 1.2%, respectively, according to Hendrickson & Teeter (1981). A novel protein from *Thermus thermophilus*, TT0570, was also used in this experiment (manuscript in preparation). TT0570 consists of 603 amino-acid residues with a molecular weight of 69 kDa and the estimated overall $\langle|\Delta F|\rangle/\langle F\rangle$ of TT0570 was 1.1% at the Cr $K\alpha$ wavelength. Crystallization experiments were all performed at 293 K using the hanging-drop vapour-diffusion method. The crystallization conditions for these proteins and the data concerning the unit-cell contents are summarized in Table 1.

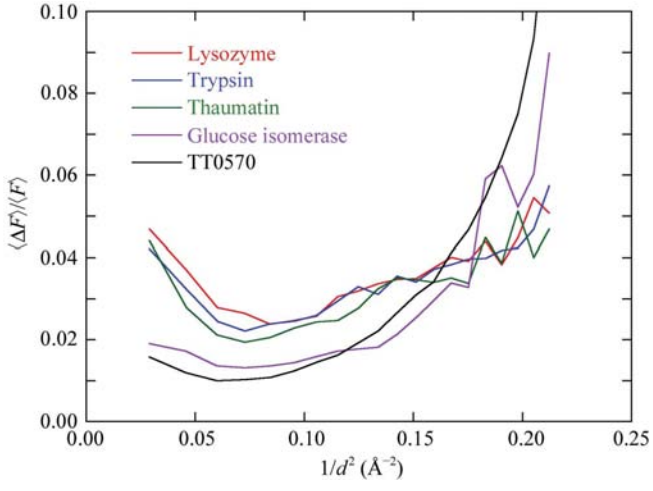

Figure 1
Amounts of anomalous signal in the diffraction data. The Bijvoet ratio $\langle|\Delta F|\rangle/\langle F\rangle$ is plotted as a function of resolution for the five test proteins.

Table 3
Solvent contents and *MLPHARE*/*DM* results.

	Lysozyme	Trypsin	Thaumatin	Glucose isomerase	TT0570
Solvent content (%)	38.2	37.9	55.7	53.7	48.0
Phase error (°)	56.5	54.5	50.1	50.0	69.7
Residues found by *ARP*/*wARP* (%)	0	16	98	89	7
Estimated $\langle\Delta F\rangle/\langle F\rangle$ (%)	5.1	4.2	2.5	1.2	1.1

The crystals were flash-cooled under a stream of nitrogen gas at 93 K after they had been transferred into a cryoprotectant solution as described in Table 1, with the exception of trypsin, which could be frozen directly. In the flash-cooling process, the crystal was mounted using a novel crystal-mounting device for eliminating X-ray absorption of buffers and cryoloops as described in Kitago *et al.* (2005). All diffraction data sets were collected using an in-house chromium X-ray source. X-rays were generated with a chromium target on a Rigaku FR-E SuperBright, which has a Cu/Cr dual target (40 kV, 40 mA for Cr), and focused through an Osmic Confocal MaxFlux optics optimized for chromium (Cr CMF). Single-pass φ-axis scan oscillation images were recorded on a Rigaku R-AXIS VII imaging-plate detector modified for using longer wavelengths (Yang *et al.*, 2003; Kitago *et al.*, 2005). A 0.5 mm collimator was used to keep the whole crystal bathed in the X-ray beam during exposure. To improve the statistics of the data sets, a total of 720 images of 1.0° oscillation were collected for lysozyme and glucose isomerase and 1440 images of 0.5° oscillation were collected for thaumatin and TT0570. In the case of trypsin, for which a relatively high Bijvoet ratio is expected from Ca^{2+} and Zn^{2+} as shown in Table 1, only 360 images of 1.0° oscillation were collected. The exposure time of each image was 1.0 min and the crystal-to-detector distance

Table 4
Comparison of three phasing methods for lysozyme.

	OASIS-2004 + *DM* + RESOLVE BUILD and/or *ARP*/*wARP* (default mode)	*SHARP* + *SOLOMON* + *ARP*/*wARP* (default mode)	*MLPHARE* + *DM* + *ARP*/*wARP*
Phase error (for top 6000 reflections) (°)	42.5	54.3	56.5
Map correlation coefficient			
Main chain	0.76	0.60	0.63
Side chain	0.65	0.52	0.49
Residues found in automatic model building			
Total No.	126	14	0
No. with side chains	126	14	0
No. of residues in ASU	129	129	129

Table 5
Comparison of three phasing methods for trypsin.

	OASIS-2004 + *DM* + RESOLVE BUILD and/or *ARP*/*wARP* (default mode)	*SHARP* + *SOLOMON* + *ARP*/*wARP* (default mode)	*MLPHARE* + *DM* + *ARP*/*wARP*
Phase error (for top 10 000 reflections) (°)	37.9	49.0	54.5
Map correlation coefficient			
Main chain	0.78	0.65	0.61
Side chain	0.72	0.62	0.56
Residues found in automatic model building			
Total No.	220	221	36
No. with side chains	220	221	7
No. of residues in ASU	223	223	223

Table 6
Comparison of three phasing methods for thaumatin.

	OASIS-2004 + *DM* + RESOLVE BUILD and/or *ARP*/*wARP* (default mode)	*SHARP* + *SOLOMON* + *ARP*/*wARP* (default mode)	*MLPHARE* + *DM* + *ARP*/*wARP*
Phase error (for top 14 000 reflections) (°)	30.3	28.4	50.1
Map correlation coefficient			
Main chain	0.77	0.77	0.63
Side chain	0.76	0.77	0.61
Residues found in automatic model building			
Total No.	203	201	203
No. with side chains	203	201	203
No. of residues in ASU	207	207	207

Table 7
Comparison of three phasing methods for glucose isomerase.

	OASIS-2004 + *DM* + RESOLVE BUILD and/or *ARP*/*wARP* (default mode)	*SHARP* + *SOLOMON* + *ARP*/*wARP* (default mode)	*MLPHARE* + *DM* + *ARP*/*wARP*
Phase error (for top 24 000 reflections) (°)	27.9	29.4	50.0
Map correlation coefficient			
Main chain	0.83	0.83	0.69
Side chain	0.76	0.77	0.60
Residues found in automatic model building			
Total No.	381	383	346
No. with side chains	381	383	312
No. of residues in ASU	388	388	388

was 80 mm. At this distance, the resolution limit at the edge of the rectangular imaging-plate detector was 2.17 Å. All data were indexed, integrated and scaled with *HKL*2000 (Otwinowski & Minor, 1997). Statistics for the diffraction data are summarized in Table 2.

2.2. Phasing and model building

For each test data set, three phasing methods, *MLPHARE* (Otwinowski, 1991), *OASIS*-2004 (Wang, Chen, Gu, Zheng, Jiang *et al.*, 2004) and *SHARP* (de La Fortelle & Bricogne, 1997), in combination with density modification were tested. For all five proteins examined, the anomalous scattering substructures were solved by *SHELXD* (Sheldrick *et al.*, 2001) and refined by *SOLVE* (Terwilliger, 1999) and the refined positions were input into *MLPHARE*, *OASIS*-2004 and *SHARP*. Only major anomalous scatterer sites from the *SHELXD* solution were used without confirming the sites with known structures. For *MLPHARE* and *OASIS*-2004, density modification was performed by *DM* (Cowtan, 1994); *SOLOMON* (Abrahams & Leslie, 1996) was used in the case of *SHARP*. Auto model-building and refinement by *ARP*/*wARP* (Perrakis *et al.*, 1999) and *REFMAC* (Murshudov *et al.*, 1997) were used to compare the resulting electron-density maps by the three phasing methods with the default mode of *CCP*4 (Collaborative Computational Project, Number 4, 1994) or *SHARP*, respectively. In the case of *OASIS*-2004, *RESOLVE* (Terwilliger, 2003*a*,*b*) was also used with the BUILD_ONLY option to find structure fragments during the early stages of iteration, because *OASIS*-2004 accepts feedback information of structure fragments found from model building and the calculation is implemented in iterative mode (Wang, Chen, Gu, Zheng & Fan, 2004). *OASIS*-2004 is an extensive revised version of the *CCP*4-supported program *OASIS* (Hao *et al.*, 2000). The latter is dedicated to *ab initio* phasing of SAD/SIR data and is based on the principle proposed by Fan & Gu (1985) and the implementation of Fan *et al.*

(1990). In the case of TT0570, combination of *SHARP*, *DM* and *ARP*/*wARP* was also tested with NCS found by *SOLVE*, because *SOLOMON* failed to find NCS for TT0570.

3. Results and discussion

3.1. Diffraction data and anomalous signals

For the five test proteins, the experimental $\langle|\Delta F|\rangle/\langle F\rangle$ is plotted as a function of resolution in Fig. 1. In the case of lysozyme and trypsin, the experimental values were lower than expected as shown in Table 1 and gave anomalous signals at the same level as thaumatin. This may have been because the expected values listed in Table 1 were calculated using all anomalous scatterers in the crystal with full occupancy. The values for lysozyme and trypsin calculated with only protein S atoms are 2.4 and 2.2%, respectively.

As a typical behaviour mentioned by Dauter *et al.* (2002), the experimental estimate of the anomalous signal became significantly higher in the high-resolution range because of the reduced accuracy of estimation of the reflection intensities. In the case of TT0570, which has a relatively low $\langle I\rangle/\langle\sigma I\rangle$ at higher resolution (Table 2), the $\langle|\Delta F|\rangle/\langle F\rangle$ plot also indicates that the quality of the data set was poorer than the others, because the experimental $\langle|\Delta F|\rangle/\langle F\rangle$ values of TT0570 increased earlier and became higher with resolution compared with the other four data sets.

3.2. SAD phasing and automated model building

The numbers of anomalous scatterer sites found by *SHELXD*, refined by *SOLVE* and used for phasing are also shown in Table 1. Using Cr $K\alpha$ radiation and our crystal-mounting method, there was no difficulty in solving anomalous scatterer substructures with *SHELXD* for all five proteins. Automatic model building by *ARP*/*wARP* using the *MLPHARE* phases after density improvement by *DM* gave 0 of 129 residues for lysozyme, 36 of 223 for trypsin, 203 of 207 for thaumatin, 346 of 388 for glucose isomerase and 87 of 1206 for TT0570. As mentioned by Ramagopal *et al.* (2003), the solvent fraction is an important factor in S-SAD phasing. The relationships between solvent content, phase error after *DM* and model building results using *ARP*/*wARP* are compiled in Table 3. With the exception of TT0570, the density-modified SAD phases were improved for the crystals with high solvent fraction and *ARP*/*wARP* could build almost all residues with a side chain. In the case of thaumatin and glucose isomerase, almost all residues were built with side chains: 203 of 207 residues and 312 of 388 residues, respectively. Conversely, in the case of lysozyme and trypsin, which have low solvent contents, model building using *ARP*/*wARP* was unsuccessful,

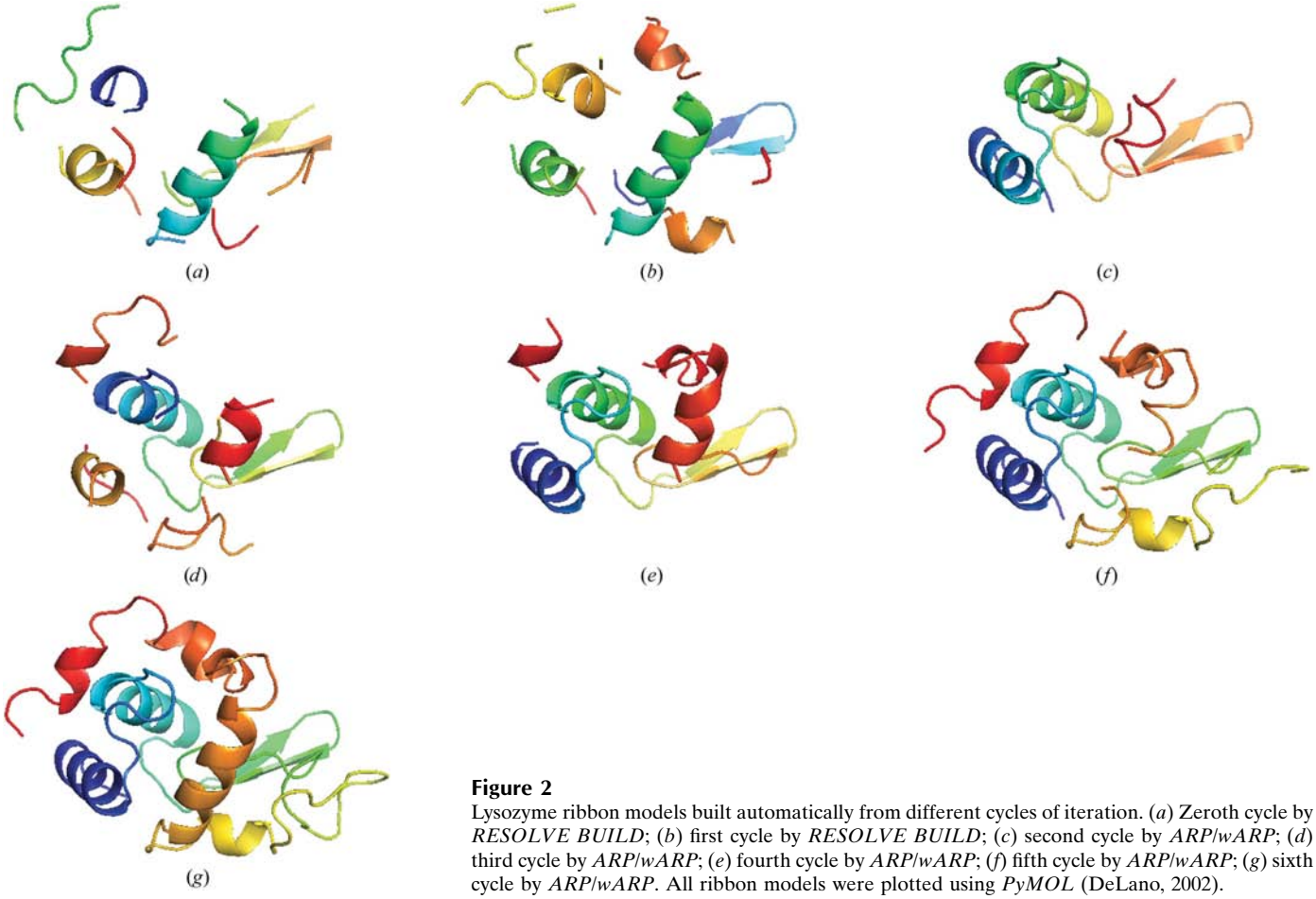

Figure 2
Lysozyme ribbon models built automatically from different cycles of iteration. (*a*) Zeroth cycle by *RESOLVE BUILD*; (*b*) first cycle by *RESOLVE BUILD*; (*c*) second cycle by *ARP*/*wARP*; (*d*) third cycle by *ARP*/*wARP*; (*e*) fourth cycle by *ARP*/*wARP*; (*f*) fifth cycle by *ARP*/*wARP*; (*g*) sixth cycle by *ARP*/*wARP*. All ribbon models were plotted using *PyMOL* (DeLano, 2002).

Table 8
Comparison of four phasing methods for TT0570.

	OASIS-2004 + *DM* + RESOLVE BUILD and/or *ARP*/*wARP* (default mode)	*SHARP* + *DM* + *ARP*/*wARP* with NCS information (manual intervention)	*SHARP* + *SOLOMON* + *ARP*/*wARP* (default mode)	*MLPHARE* + *DM* + *ARP*/*wARP*
Phase error (for top 66 000 reflections) (°)	49.7	56.7	60.7	69.7
Map correlation coefficient				
Main chain	0.70	0.64	0.58	0.48
Side chain	0.61	0.55	0.47	0.38
Residues found in automatic model building				
Total No.	1173	1117	340	87
No. with side chains	1167	964	17	0
No. of residues in ASU	1206	1206	1206	1206

even though the experimental anomalous signal of $\langle|\Delta F|\rangle/\langle F\rangle$ seemed sufficient as shown in Fig. 1.

Detailed comparisons of the results of three phasing methods for each test protein are shown in Tables 4, 5, 6, 7 and 8. In all cases, *SHARP*/*SOLOMON* and *OASIS*-2004/*DM* gave better results than *MLPHARE*/*DM*. A clear difference between *SHARP* and *OASIS*-2004 was seen in the two difficult cases of lysozyme and TT0570. In both cases, *OASIS*-2004 gave better results than *SHARP*, even if the NCS information was used for density improvement with *DM* (Table 8). As shown in Tables 4–8, in the case of proteins with sufficient sulfur contents almost all of the structure could be constructed in a straightforward manner by *OASIS*-2004: 126 of 129 residues (97.7%) for lysozyme, 220 of 223 (98.7%) for trypsin, 203 of 207 (98.1%) for thaumatin, 381 of 388 (98.2%) for glucose isomerase and 1173 of 1206 (97.3%) for TT0570. The superiority of *OASIS*-2004 arises from its implemented fragment feedback in the direct-method probability calculation (Wang, Chen, Gu, Zheng & Fan, 2004). No manual intervention was needed to tune controlling parameters during either the phase derivation or automatic model building. As an example, ribbon models built automatically at different cycles of iteration for lysozyme are shown in Fig. 2. The numbers of residues found in each cycle of iteration of *OASIS*-2004 are shown in Table 9.

4. Conclusions

The results of the present study show that the solvent contents are still an important factor for phasing with the S-SAD method, even when longer wavelength Cr $K\alpha$ radiation is used. Among the three phasing procedures, the improved direct phasing by *OASIS*-2004 with its implemented fragment feedback in the direct-method probability calculation gave the best results in determining the initial phases.

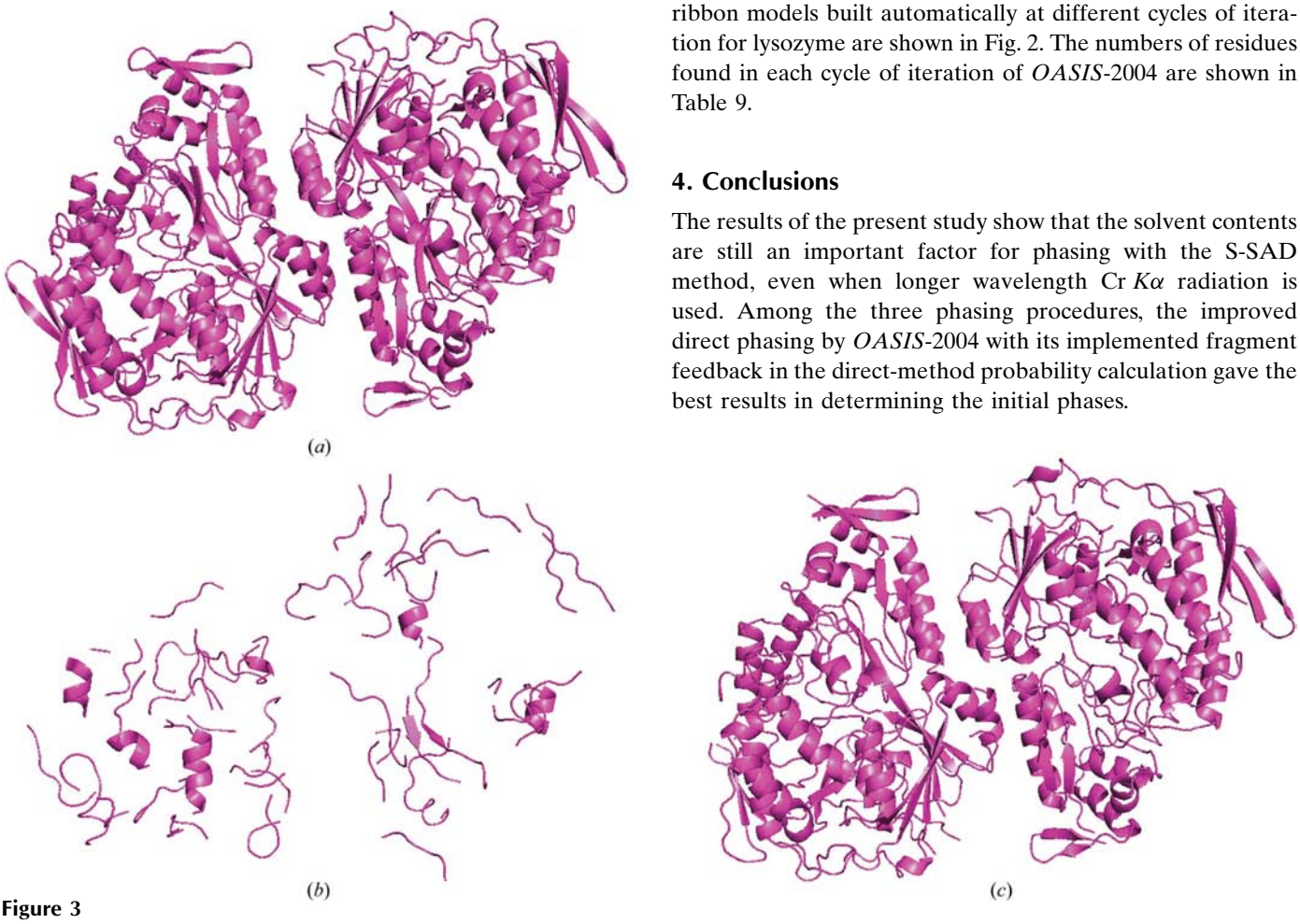

Figure 3
TT0570 ribbon models built automatically using different phasing methods. (*a*) *OASIS*-2004 with *DM*; (*b*) *SHARP* with *SOLOMON*; (*c*) *SHARP* with *DM* using NCS information. All ribbon models were plotted using *PyMOL* (DeLano, 2002).

Table 9
No. of residues found automatically in each cycle of *OASIS*-2004 iteration.

A, model built by *ARP*/*wARP* with *CCP*4 default mode. R, model built by *RESOLVE* with BUILD_ONLY mode.

Sample	Lysozyme	Trypsin	Thaumatin	Glucose isomerase	TT0570
Residues in the ASU	129	223	207	388	1206
Residues found in each cycle					
Cycle 0	67 (R)	113 (R)	57 (R)	281 (R)	838 (R)
Cycle 1	78 (R)	109 (R)	99 (A)	381 (A)	881 (R)
Cycle 2	65 (A)	188 (A)	191 (A)		1167 (A)
Cycle 3	79 (A)	213 (A)	203 (A)		
Cycle 4	80 (A)	220 (A)			
Cycle 5	117 (A)				
Cycle 6	126 (A)				

In the present study, we applied this Cr S-SAD method to a larger target, TT0570, which has a molecular weight of 69 kDa and crystallizes in the orthorhombic space group $P2_12_12$. The crystal contains two independent molecules in the asymmetric unit, which corresponds to 1206 residues per asymmetric unit. Furthermore, it has a relatively low sulfur content, with nine Met and two Cys residues per molecule and a calculated Bijvoet ratio corresponding to 1.1% even with the use of Cr $K\alpha$ radiation (or 0.57% for Cu $K\alpha$ radiation). Reflecting these characteristics, the data statistics of TT0570 were much poorer than those for the other standard proteins examined here (Table 2). The overall signal-to-noise ratio of the anomalous differences $\langle|\Delta F|\rangle/\langle\sigma(\Delta F)\rangle$ for TT0570 was only 0.80. Nonetheless, the structure could be solved by the S-SAD method using *OASIS*-2004. Although TT0570 has a solvent content of 48% and the data had poor statistics compared with the other test proteins, the electron-density map was sufficiently clear to allow protein models to be built (Fig. 3). As shown in Table 8, 1173 of 1206 residues (97.3%) were constructed in a straightforward manner.

High-throughput crystallography in the post-genomic era requires a method by which the native protein structure can be solved both quickly and easily. Several phasing techniques exploiting anomalous signals in the data collected with in-house generators have emerged in recent years. The MAD method using SeMet substitution is no longer the only solution. The present results showed that the combination of our loopless data-collection method using Cr $K\alpha$ radiation and the *OASIS*-2004 phasing method with density modification is a powerful and routine tool to solve novel structures with the S-SAD method.

This study was supported in part by a research grant from the National Project on Protein Structural and Functional Analysis from the Ministry of Education, Culture, Sports, Science and Technology of Japan and by the Innovation Project of the Chinese Academy of Sciences and the 973 Project (Grant No. 2002CB713801) and the 863 Project (Grant No. 2002BA711A12) of the Ministry of Science and Technology of China.

References

Abrahams, J. P. & Leslie, A. G. W. (1996). *Acta Cryst.* D**52**, 30–42.
Blow, D. M. (1958). *Proc. R. Soc. London Ser. A*, **247**, 302–336.
Chayen, N. E., Cianci, M., Olczak, A., Raftery, J., Rizkallah, P. J., Zagalsky, P. F. & Helliwell, J. R. (2000). *Acta Cryst.* D**56**, 1064–1066.
Chen, L., Chen, L, Zhou, X. E., Wang, Y., Kahsai, M. A., Clark, A. T., Edmondson, S. P., Liu, Z., Rose, J. P., Wang, B.-C., Meehan, E. J. & Shriver, J. W. (2004). *J. Mol. Biol.* **341**, 73–91.
Cianci, M., Rizkallah, P. J., Olczak, A., Raftery, J., Chayen, N. E., Zagalsky, P. F. & Helliwell, J. R. (2001). *Acta Cryst.* D**57**, 1219–1229.
Collaborative Computational Project, Number 4 (1994). *Acta Cryst.* D**50**, 760–763.
Cowtan, K. (1994). *Jnt CCP4/ESF–EACBM Newsl. Protein Crystallogr.* **31**, 34–38.
Dauter, Z., Dauter, M. & Dodson, E. J. (2002). *Acta Cryst.* D**58**, 494–506.
Dauter, Z., Dauter, M. & Rajashankar, K. R. (2000). *Acta Cryst.* D**56**, 232–237.
DeLano, W. L. (2002). *The PyMOL Molecular Graphics System.* DeLano Scientific, San Carlos, CA, USA.
Evans, G. & Bricogne, G. (2002). *Acta Cryst.* D**58**, 976–991.
Fan, H.-F. & Gu, Y.-X. (1985). *Acta Cryst.* A**41**, 280–284.
Fan, H.-F., Hao, Q., Gu, Y.-X., Qian, J.-Z., Zheng, C.-D. & Ke, H. (1990). *Acta Cryst.* A**46**, 935–939.
Hao, Q., Gu, Y.-X., Zheng, C.-D. & Fan, H.-F. (2000). *J. Appl. Cryst.* **33**, 980–981.
Hendrickson, W. A. (1985). *Trans. Am. Crystallogr. Assoc.* **21**, 11–21.
Hendrickson, W. A. & Teeter, M. M. (1981). *Nature (London)*, **290**, 107–113.
Jáuregui, R., Bolivar, F. & Merino, E. (2000). *Microb. Comput. Genomics*, **5**, 7–15.
Kitago, Y., Watanabe, N. & Tanaka, I. (2005). *Acta Cryst.* D**61**, 1013–1021.
La Fortelle, E. de & Bricogne, G. (1997). *Methods Enzymol.* **276**, 472–494.
Liu, Z.-J., Vysotski, E. S., Chen, C.-J., Rose, J. P., Lee, J. & Wang, B.-C. (2000). *Protein Sci.* **9**, 2085–2093.
Madauss, K., Juzumiene, D., Waitt, G., Williams, J. & Williams, S. (2004). *Endocrine Res.* **30**, 775–785.
Micossi, E., Hunter, W. N. & Leonard, G. A. (2002). *Acta Cryst.* D**58**, 21–28.
Mueller-Dieckmann, C., Panjikar, S., Tucker, P. A. & Weiss, M. (2005). *Acta Cryst.* D**61**, 1263–1272.
Mueller-Dieckmann, C., Polentarutti, M., Djinovic Carugo, K., Panjikar, S., Tucker, P. A. & Weiss, M. (2004). *Acta Cryst.* D**60**, 28–38.
Murshudov, G. N., Vagin, A. A. & Dodson, E. J. (1997). *Acta Cryst.* D**53**, 240–255.
Nagem, R. A., Ambrosio, A. L., Rojas, A. L., Navarro, M. V., Golubev, A. M., Garratt, R. C. & Polikarpov, I. (2005). *Acta Cryst.* D**61**, 1022–1030.
Nagem, R. A., Dauter, Z. & Polikarpov, I. (2001). *Acta Cryst.* D**57**, 996–1002.
Otwinowski, Z. (1991). *Proceedings of the CCP4 Study Weekend. Isomorphous Replacement and Anomalous Scattering*, edited by W. Wolf, P. R. Evans & A. G. W. Leslie, pp. 80–86. Warrington: Daresbury Laboratory.
Otwinowski, Z. & Minor, W. (1997). *Methods Enzymol.* **276**, 307–326.
Perrakis, A., Morris, R. & Lamzin, V. S. (1999). *Nature Struct. Biol.* **6**, 458–463.
Phillips, J. D., Whitby, F. G., Warby, C. A., Labbe, P., Yang, C., Pflugrath, J. W., Ferrara, J. D., Robinson, H., Kushner, J. P. & Hill, C. P. (2004). *J. Biol. Chem.* **279**, 38960–38968.
Ramagopal, U. A., Dauter, M. & Dauter, Z. (2003). *Acta Cryst.* D**59**, 1020–1027.
Rice, L. M., Earnest, T. N. & Brunger, A. T. (2000). *Acta Cryst.* D**56**, 1413–1420.

Rose, J. P., Liu, Z.-J., Tempel, W., Chen, D., Lee, D., Newton, M. G. & Wang, B.-C. (2004). *Rigaku J.* **21**, 1–9.
Sheldrick, G. M., Hauptman, H. A., Weeks, C. M., Miler, M. & Usón, I. (2001). *International Tables for Crystallography*, Vol. *F*, edited by E. Arnold & M. G. Rossmann, pp. 333–351. Dordrecht: Kluwer Academic Publishers.
Stuhrmann, S., Hütsch, M., Trame, C., Thomas, J. & Stuhrmann, H. B. (1995). *J. Synchrotron Rad.* **2**, 83–86.
Teplyakov, A., Oliva, G. & Polikarpov, I. (1998). *Acta Cryst.* D**54**, 610–614.
Terwilliger, T. C. (1999). *Acta Cryst.* D**55**,1863–1871.
Terwilliger, T. C. (2003*a*). *Acta Cryst.* D**59**, 38–44.
Terwilliger, T. C. (2003*b*). *Acta Cryst.* D**59**, 45–49.
Usón, I., Schmidt, B., von Bulow, R., Grimme, S., von Figura, K., Dauter, M., Rajashankar, K. R., Dauter, Z. & Sheldrick, G. M. (2003). *Acta Cryst.* D**59**, 57–66.
Wang, B.-C. (1985). *Methods Enzymol.* **115**, 90–112.
Wang, J.-W., Chen, J.-R., Gu, Y.-X., Zheng, C.-D. & Fan, H.-F. (2004). *Acta Cryst.* D**60**, 1991–1996.
Wang, J.-W., Chen, J.-R., Gu, Y.-X., Zheng, C.-D., Jiang, F. & Fan, H.-F. (2004). *Acta Cryst.* D**60**, 1987–1990.
Weiss, M. S. & Hilgenfeld, R. (1997). *J. Appl. Cryst.* **30**, 203–205.
Weiss, M. S., Sicker, T., Djinovic Carugo, K. & Hilgenfeld, R. (2001). *Acta Cryst.* D**57**, 689–695.
Xu, H., Yang, C., Chen, L., Kataeva, I. A., Tempel, W., Lee, D., Habel, J. E., Nguyen, D., Pflugrath, J. W., Ferrara, J. D., Arendall, W. B. III, Richardson, J. S., Richardson, D. C., Liu, Z.-J., Newton, M. G., Rose, J. P. & Wang, B.-C. (2005). *Acta Cryst.* D**61**, 960–966.
Yang, C., Pflugrath, J. W., Courville, D. A., Stence, C. N. & Ferrara, J. D. (2003). *Acta Cryst.* D**59**, 1943–1957.